Nano Biomed Eng
2018, 10(3): 199-212. doi: 10.5101/nbe.v10i3.p199-212.

Research Article

Synthesis and Biological Screening of the Gold Complex as Anticancer and Some Transition Metal Complexes with New Heterocyclic Ligand Derived from 4-Amino Antipyrine

Layla Ali Mohammed, Raheem Tahir Mehdi, Abid Allah Mohammed Ali

Department of Chemistry, College of Education for Girls, University of Kufa, Iraq.

Corresponding author. E-mail: laila.alameri@uokufa.edu.iq

Received: Mar. 20, 2018; **Accepted:** Jun. 3, 2018; **Published:** Jul. 10, 2018.

Citation: Layla Ali Mohammed, Raheem Tahir Mehdi, and Abid Allah Mohammed Ali, Synthesis and Biological Screening of the Gold Complex as Anticancer and Some Transition Metal Complexes with New Heterocyclic Ligand Derived from 4-Amino Antipyrine. *Nano Biomed. Eng.*, 2018, 10(3): 199-212.
DOI: 10.5101/nbe.v10i3.p199-212.

Abstract

A new azo Schiff-base ligand, (N^1Z,N^2Z)-N^1,N^2-bis(4-((Z)4-hydroxy naphthalen-1-yl)diazenyl)-(1,5-dimethy-2-phenyl-1H-pyrazol-3(2H)-ylidene) benzene-1,2-diamine, has been synthesized from coupling (N^1Z,N^2Z)-N^1,N^2-bis(4-amino-1,5-dimethyl-2-phenyl-1H-pyrazol-3(2H)-ylidene)benzene-1,2-diamine with 1-naphthol. Fourier-transform infrared spectroscopy (FTIR), proton nuclear magnetic resonance (^{1}H-NMR), carbon nuclear magnetic resonance (^{13}C-NMR) technique, ultraviolet-visible spectroscopy (UV-Vis), mass analysis, molar conductance and magnetic susceptibility were used to characterize the structures of the new ligand and their transition metal complexes. The complexes were found to have the general formula $(M)(L)Cl_2$ where M = Co(II), Ni(II), Cu(II), Zn(II), Cd(II) and Hg(II), $(M)(L)Cl_3$ where M = Au(III), and $(M)(L)Cl_2Cl$ where M = Fe(III). The FTIR results demonstrated that the coordination sites were the azomethine nitrogen and azo nitrogen atoms of the azo Schiff-base ligand. The electronic spectral and magnetic measurement data indicated that the complexes exhibited octahedral geometry, except the Au(III) complex suggested a square planar geometry around the central metal ion. The results showed the highest inhibitory effect for gold the complex. The effect of biological screening of the gold complex on human colon cancer cell line LS-174 was investigated. The gold complex was observed to have the highest inhibitory effect.

Keywords: 4-Amino antipyrine; Azo Schiff-base; Transition metal complexes; Antitumor activity

Introduction

A great deal of work has been reported on the synthesis and characterization of different types of azo Schiff bases. Due to the excellent donor properties of the azo and azomethine groups, these compounds present one important field in coordination chemistry [1, 2]. In addition to their interesting coordination properties, azo Schiff-base metal complexes have been studied extensively for years due to the synthetic flexibilities of these Schiff-base ligands and their selectivity as well as sensitivity towards the transition metal ions, and that their complexes have important biological activities [3], redox and catalytic properties

[4], corrosion inhibition [5], and antimicrobial reagent [6]. 4-aminoantipyrine heterocyclic compound has gained great importance as it is abundant in nature and wide pharmacological activities. 4-aminoantipyrine is a pyrazole derivative which has antipyretic action. It is used in the preparation of azo dyes [7] and Schiff base [8], also used to protect against oxidative effect as well as prophylactic of certain diseases including cancer [9]. Several derivatives of antipyrine were also evaluated as analgesic [10], anti-inflammatory [11], antimicrobial [12] and anticancer [13]. The aim of this paper is to synthesize, characterize and study the biological screening of the gold complex as anticancer of the new tetra dentate azo Schiff-base ligand, (N^1Z,N^2Z)-N^1,N^2-bis(4-((Z)4-hydroxy naphthalen-1-yl)diazenyl)-(1,5-dimethy-2-phenyl-1H-pyrazol-3(2H)-ylidene) benzene-1,2-diamine and some of its transition metal complexes.

Experimental

Materials

All chemicals were supplied by BHD and Sigma Aldrich, Germany, and used without further purification.

Measurement

The electro-thermal melting point model 9300 was used to measure the melting point of the ligand and its complexes. Elemental analyses were carried out by means of micro analytical unit of 1180 C.H.N elemental analyzer. Electronic spectra were recorded on Shimadzu spectrophotometer double beam model 1700 ultraviolet-visible (UV-Vis) spectrophotometer. Fourier-transform infrared (FTIR) spectra were recorded in KBr disc on FTIR Shimadzu spectrophotometer model 8400 in wave number 4000-400/cm. Proton nuclear magnetic resonance (^{1}H-NMR) and carbon nuclear magnetic resonance (^{13}C-NMR) spectra in ppm unit were operating in dimethyl sulfoxide-d6 (DMSO-d6) as solvent using (Bruker Ultra Shield 3000 MHz, Switzerland). And mass spectra were recorded on AB Sciex 3200 QTRAP LC/MS/MS (mass range m/z 5-2000 quad mode and 50-1700 linear ion trap mode). Magnetic susceptibility measurements were carried out on a balance magnetic MSB-MKI using faraday method. The diamagnetic corrections were made by Pascal's constants.

Preparation of the azo Schiff-base ligand

Preparation of the Schiff base

The Schiff base ligand was prepared by condensation of 1.08 g, 0.01 mol o-phenylene diamine with 4.064 g, 0.02 mol 4-amino antipyrine at 1 : 2 mole ratio, in absolute alcohol. A few drops of glacial acetic acid were added to the reaction mixture and refluxed with stirring for 35 h. With the precipitate product collected by filtering off, the resulting solution was evaporated to half volume, purified by crystallization from hot ethanol, and dried over anhydrous $CaCl_2$. Yield = 88%; melting point (MP) = 125-127 °C (Scheme 1).

Preparation of the azo Schiff-base ligand

The new azo Schiff-base ligand was prepared by coupling reaction of diazonium salt with appropriate amount of 1-naphthol as coupling component in alkaline solution. Diazonium solution was prepared by dissolving 4.78 gm, 0.01 mol (N^1Z,N^2Z)-N^1,N^2-bis(4-amino-1,5-dimethyl-2-phenyl-1H-pyrazol-3(2H)-ylidene)benzene-1,2-diamine in 4 mL concentrated hydrochloric acid and 30 mL distilled water. To this mixture a solution of 1.4 gm, 0.02 mol sodium nitrate in 10 mL distilled water was added dropwise at 0-5 °C, and left to stand 30 min. This diazonium solution was added dropwise to 1-naphthol (2.88 gm, 0.02 mol) dissolved in 50 mL ethanol and 60 mL sodium hydroxide (2N) at 0-5 °C. The mixture was allowed to stand overnight. The precipitate was filtered off, washed with distilled water, and recrystallized twice from hot ethanol and then dried in oven at 50 °C for 12 h. MP = 173-175 °C; yield = 80% (Scheme 2).

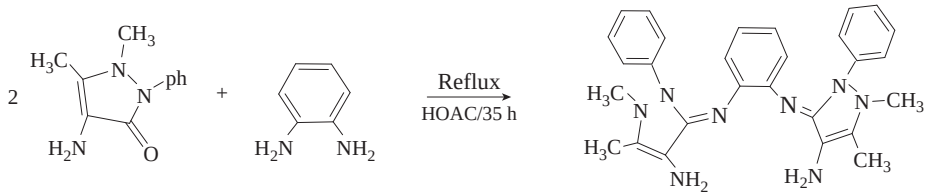

4-amino antipyrine o-phenylenediamine

(N^1Z,N^2Z)-N^1,N^2-bis(4-amino-1,5-dimethyl-2-phenyl-1H-pyrazol-3(2H)-ylidene)benzene-1,2-diamine

Scheme 1 Preparation of the Schiff-base ligand.

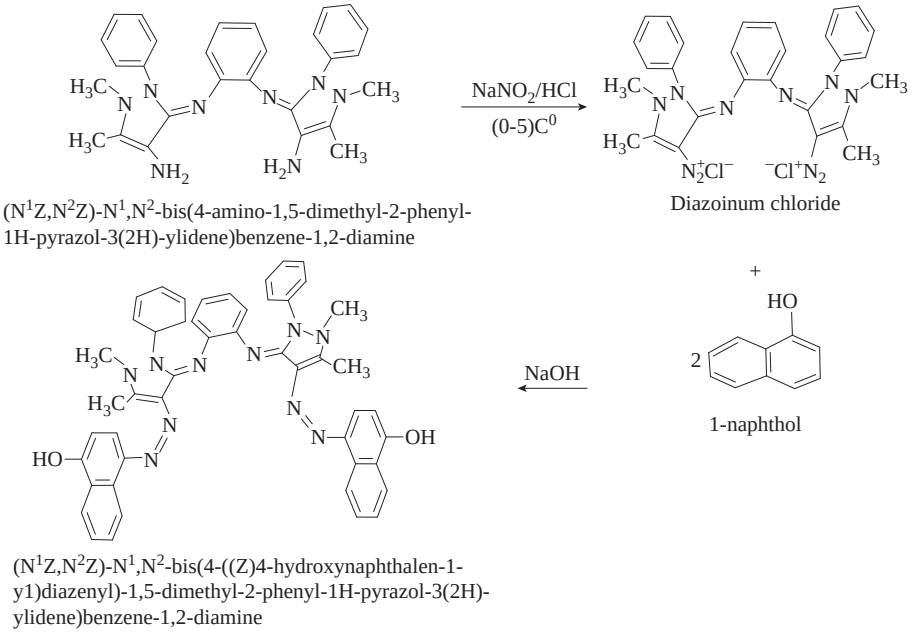

(N^1Z,N^2Z)-N^1,N^2-bis(4-amino-1,5-dimethyl-2-phenyl-1H-pyrazol-3(2H)-ylidene)benzene-1,2-diamine

Diazoinum chloride

(N^1Z,N^2Z)-N^1,N^2-bis(4-(((Z)4-hydroxynaphthalen-1-y1)diazenyl)-1,5-dimethyl-2-phenyl-1H-pyrazol-3(2H)-ylidene)benzene-1,2-diamine

Scheme 2 Preparation of the azo Schiff-base ligand.

Preparation of metal complexes

The metal complexes were prepared by mixing 25 mL ethanol solution of $FeCl_3\,2H_2O$, $CoCl_2\,6H_2O$, $NiCl_2\,6H_2O$, $CuCl_2\,2H_2O$, $ZnCl_2$, $CdCl_2\,2H_2O$, $HgCl_2\,2H_2O$, $NaAuCl_4\,H_2O$ with 25 mL ethanol solution of azo Schiff-base ligand in 1 : 1 (metal : ligand) ratio. The resulting mixture was refluxed for 1 h. The product was isolated after the volume was reduced by evaporation. It was filtered off, washed with ethanol and dried under vacuum. The complexes obtained are listed in Table 2.

Biological part

All chemicals and biological materials were supplied from Sigma, Difco, USA, Santacruze Biotechnology Inc, Europe, BDH, Flow Laboratories, GCC, UK, and Merk, Germany). Instruments were supplied from Arnold Sons, Genex, Beckman Model J2-21, Lab-TeK and Nunc, USA, Memmert, Hermle, Leica, Sartorius, Leitz, Germany, Marubeni, Ogawa Seiki, Japan, Gallen-Kamp, UK, Eppendroff, Oxford, LKB, Sweden, and Nunc, Denmark.

Cell culture media

Two types of cell culture media were used in this assay: Growth media (GM) and maintenance media (MM). The pH was checked and adjusted to about 6.8-7.1. The antibiotics were added to culture medium at final concentration of 100 IU/mL and 100 µg/mL of penicillin G and streptomycin, respectively (1 mL antibiotic solution to 100 mL culture medium). Nystatin was also added to give the final concentration of 25 IU/mL. Filtration of media was carried out in biohazard safety cabinet using 0.22 µm Millipore filter. To prepare 100 mL GM and MM, the components were mixed up to prepare media necessary for LS-174 cell line revealed in Table 1.

Table 1 Constituents of cell culture media for LS-174 cell line

Components	Growth media (mL)	Maintenance media (mL)
1X RPMI 1640	84.5	91.5
HEPES 1M	2	2
Fetal calf serum (FCS)	10	2
--	1	1
Nystatin	1	1
$NaHCO_3$ (7.5%) solution	1.5	2.5

Each bottle was sealed tightly, labeled with name, date, and kept in incubator at 37 °C. The bottles were examined after 2-3 days later. If there were no turbidity and no indication of bacterial growth, they would be transferred to refrigerator to store till use.

Cytotoxicity assay

Cell lines were seeded onto 96 well plates with a concentration of 1.0×10^5 cells/mL. After incubation at 37 °C for 24 to 48 h, the confluent monolayer of LS-174 cells was complete (80-100%). Different concentrations (0.5, 1, 10, 100, 1000, 2000, 3000, 4000, 5000 and 10000 µg/mL) of micro tittered Au(III) complex were added to cultured wells at a final volume of 100 µL in each well except control cells in triplicate. After 24 h, incubation at 37 °C in 5% CO_2, the micro

titer 96 wells plates were marched out and transferred to biohazard safety cabinet in sterilized environment to avoid any contamination. All used wells media were discarded. The LS-174 cell monolayers were washed by phosphate buffered saline (PBS) solution to remove any residual amount of complexes or standard anticancer drug used that might interact with methyl thiazolyl tetrazolium (MTT) reagents. Then, 100 µL maintenance media was added to all wells containing drug treated cells and drug untreated cells, and blank wells. Then, MTT reagent (20 µL) was added to each well. After 4 h of incubation at 37 °C and 5% CO_2, the formazan particles were formed as a mitochondrial enzymatic process of the non-effected viable LS-174 cells. Dead or viral effected cells didn't form formazan particles because their mitochondria organelles were disrupted. The formazan was dissolved by adding diluted DMSO: isopropanol at 1 : 1 ratio on each well including blank wells. The absorbance was read at 490 nm with a reference wavelength of 630 nm by an ELISA reader. This protocol of MTT assay measurement was mentioned by many reports [14, 15]. Mean blank absorption was subscribed from other samples and control well absorptions.

Results and Discussion

All our complexes were stable in air. They were freely soluble in DMSO, dimethylformamide (DMF), methanol and ethanol. The metal complexes were characterized by elemental analysis, molar conductivity, FTIR, UV-Vis and ^{1}H-MNR spectroscopy. The analytical data of the complexes were in agreement with the experimental data (Table 2). The value revealed that the metal to ligand ratio was 1 : 1. The magnetic susceptibility of the chelate complexes at room temperature was consistent with octahedral geometry, except the Au(III) complex suggested a square planar geometry around the central metal ion. Most of the chelate complexes prepared in this work showed lower conductivity values compared to Au and Fe complexes. This proved that complexes had non-electrolytic nature, except the Au(III) and Fe(III) complexes which showed higher conductivity values supported the electrolytic nature of the metal complexes.

Micro analysis

The elemental analysis data of 1 : 1 metal : ligand (M : L) ratio complexes showed that the theoretical values were in good agreement with the found data, as listed in Table 2. The purity of azo Schiff-base ligand was tested by thin-layer chromatography (TLC) technique and CHN elemental analysis.

Infrared spectra studies of the ligand and its complexes

The FTIR spectra provided valuable information regarding the nature of the functional group attached to the metal atom. The most important infrared spectral bands that provided conclusive structural evidence for the coordination of the ligand to the central metal ions are given in Table 3. The FTIR spectrum of the ligand showed characteristic bands at 3419, 1639 and 1450/cm due to the O-H, C=N and N=N functional groups, respectively [16]. The IR spectra of the ligand exhibited appropriate shifts due to the formation of

Table 2 Physical properties and elemental analysis of azo Schiff-base ligand and their metal complexes

Compound	C (%) Cal. /found	H (%) Cal. /found	N (%) Cal. /found	M (%) Cal. /found	MP (°C)	M .Wt (gm/mol)	Color	Yield (%)
$C_{48}H_{40}N_{10}O_2$ = L	73.09/72.94	5.07/5.01	15.22/15.08	--	173-175	788	Deep-red	80
$Cu(L)Cl_2$	62.44/61.56	4.33/4.21	15.17/15.06	6.88/6.57	>310	922.4	Violet-reddish	85
$Ni(L)_{C}l2$	62.76/61.87	4.35/4.22	15.25/15.18	6.39/6.25	>310	917.7	purple	72
$Co(L)Cl_2$	62.75/61.84	4.35/4.13	15.25/14.99	6.41/6.09	>310	917.9	Violet-reddish	62
$Zn(L)Cl_2$	62.31/62.01	3.69/3.18	15.14/14.89	7.07/6.88	140-141	924.3	Violet-reddish	75
$Cd(L)Cl_2$	59.29/58.66	4.11/4.09	14.41/13.96	11.57/10.76	238-240	971.4	Violet-reddish	72
$Hg(L)Cl_2$	54.36/53.86	3.77/13.21	13.21/12.79	18.92/18.12	260-262	1059.5	purple	70
$Fe(L)Cl_2Cl$	60.61/59.76	4.20/4.04	14.73/14.19	5.87/5.21	>310	950.3	Violet-reddish	78
$Au(L)Cl_3$	52.77/52.21	3.66/3.46	12.82/12.22	18.04/17.92	128-130	1091.4	Violet-reddish	82

Note: Cal. = calculated; M .Wt = molecular weight.

Table 3 Characteristic IR absorption bands of the ligand and its complexes

Compound	υ(O-H)/cm	υ(N=N)/cm	υ(C=N)/cm	υ(N-N)/cm	υ(M-N)/cm
H(L)	3419	1450	1639	1028	--
$Cu(L)_Cl2$	3419	1406	1627	1022	449
$Co(L)Cl_2$	3406	1409	1625	1024	449
$Ni(L)Cl_2$	3412	1427	1620	1022	449
$Fe(L)Cl_2Cl$	3419	1435	1625	1022	430
$Zn(L)Cl_2$	3412	1444	1627	1024	464
$Cd(L)Cl_2$	3415	1409	1612	1024	428
$Hg(L)Cl_2$	3423	1409	1630	1028	432
$Au(L)Cl_3$	3400	1402	1627	1024	447

all complexes prepared in this study. The C=N and N=N bands in the free ligand shifted from 1639-1450/cm to 1630-1612/cm and 1444-1402/cm, respectively for the complexes. The reduction in bond order, upon complexion, could be attributed to the delocalization of metal electron density (t_2g) to the -system of the ligand. These shifts confirmed the coordination of the ligand via the nitrogen of azo methine and the azo groups to metal ions [17]. The absorption band in free ligand observed at 3419/cm was attributed to the υ(OH) of hydroxyl group [18]. This band remained unchanged in the spectra of their complexes, which suggested that the hydroxyl group was not taking part in coordination [19]. New bands were attributed to υ(M-N) vibrations appearance in all complexes at 449-428/cm, respectively [20]. The stretching wave number due to N-N in the coordinated compound was slightly affected from 1024/cm, which indicated the unsharing of this linkage of pyrazolone ring in coordination with metal ions [21]. Representative example for their spectra is given in Fig. 1.

Mass spectra

The mass spectra of synthesized azo Schiff-base ligand and its Cu(II) complex were recorded at room temperature. The obtained molecular ion peaks confirmed the proposed formulae for the synthesized compounds. The mass spectrum of the ligand shows the molecular ion peak at m/z 788.8 for the compound $C_{48}H_{40}N_{10}O_2$, confirming the proposed formula for the

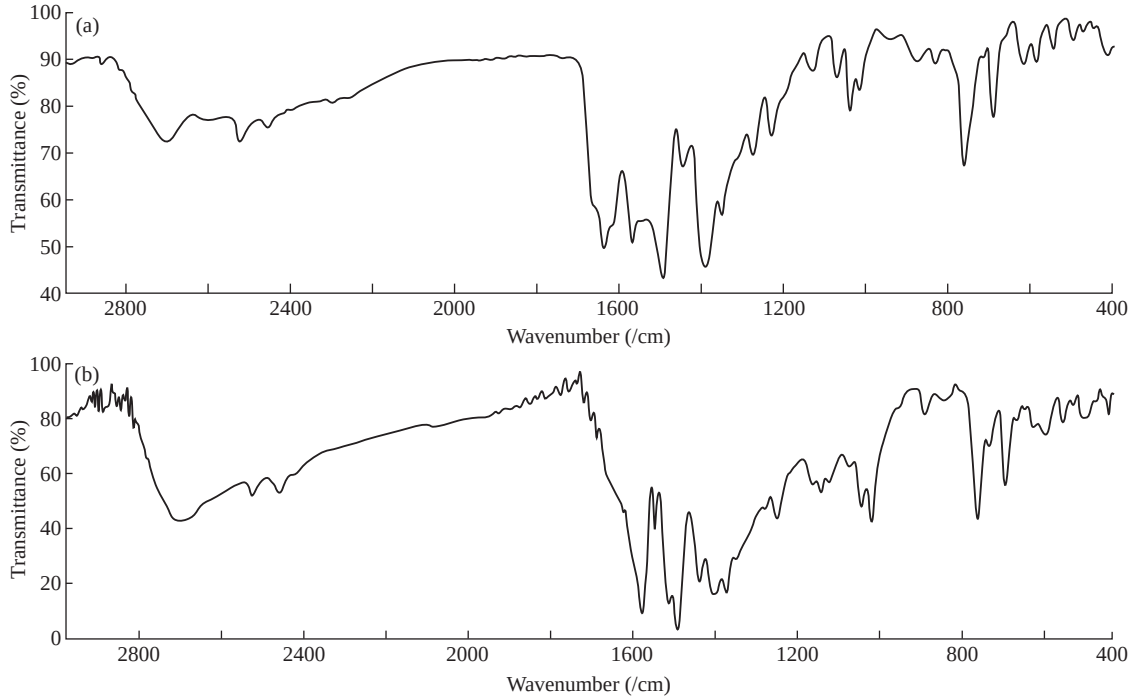

Fig. 1 FTIR spectra of **(a)** azo Schiff-base ligand and **(b)** Cu (II) complex.

synthesized compound. Also The mass spectrum of the Cu(II) complex exhibited the molecular ion peak at m/z 922.5 for the molecular formula $Cu(C_{48}H_{40}N_{10}O_2)Cl_2$, which was consistent with the molecular weight of the Cu(II) complex and in good agreement with their formula as expressed from micro analytical data. The mass spectral data fragmentation of the ligand and Cu(II)-complex are shown in Scheme 3, 4, and Fig. 2.

^{1}H-NMR spectra

The ^{1}H-NMR spectrum of the ligand showed the following signals: Phenyl multiples at 6.8-8.7 ppm, =C-CH_3 at 2.7 ppm, -N-CH_3 at 3.3 ppm, and -OH at 10.6 ppm [6, 22]. This peak was noted in the spectra of complexes indicated that the –OH proton did not contribute to the complexity. There was no appreciable change in all other signals in the complexes, as shown

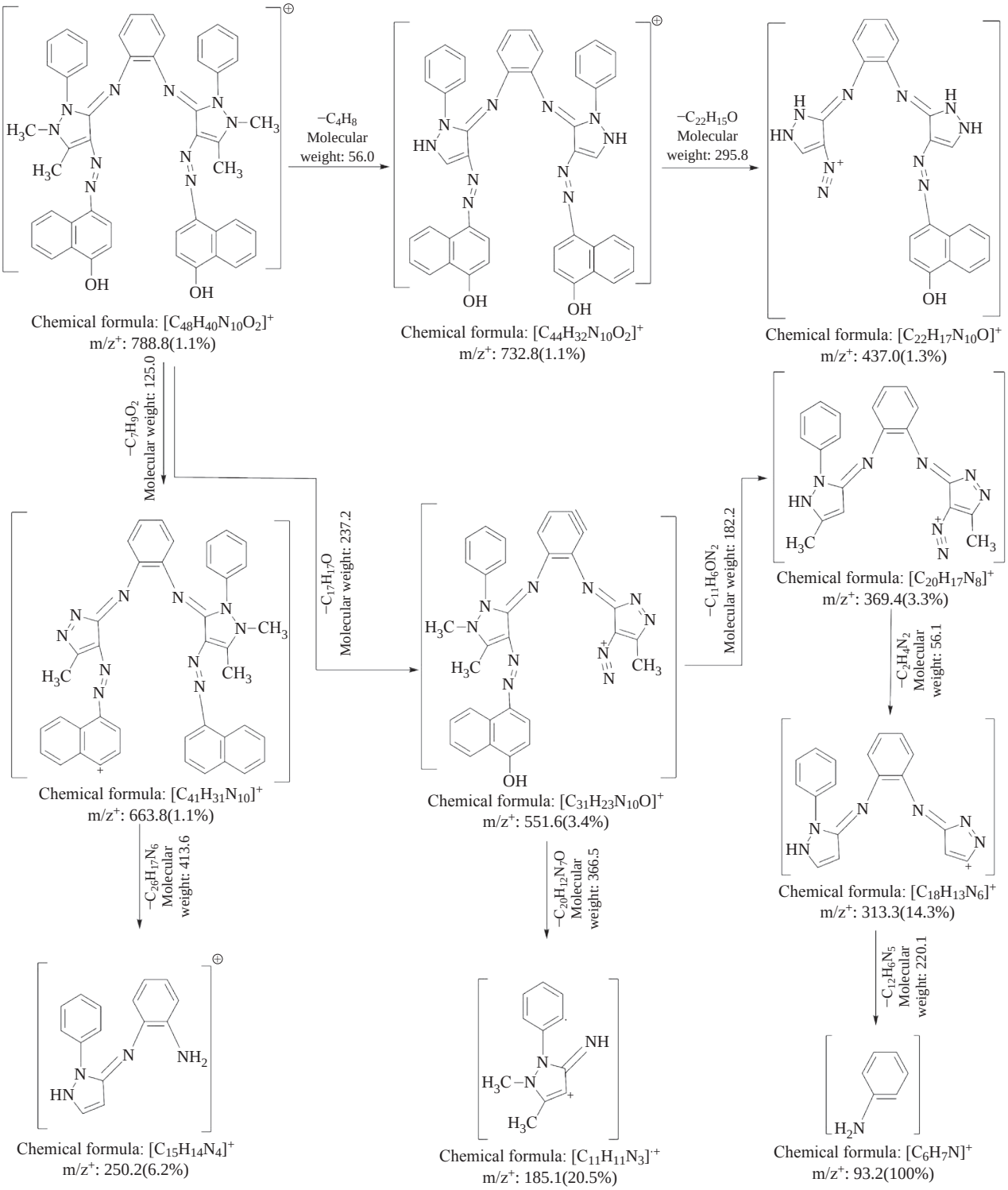

Scheme 3 Mass spectrum fragmentation of azo Schiff-base ligand.

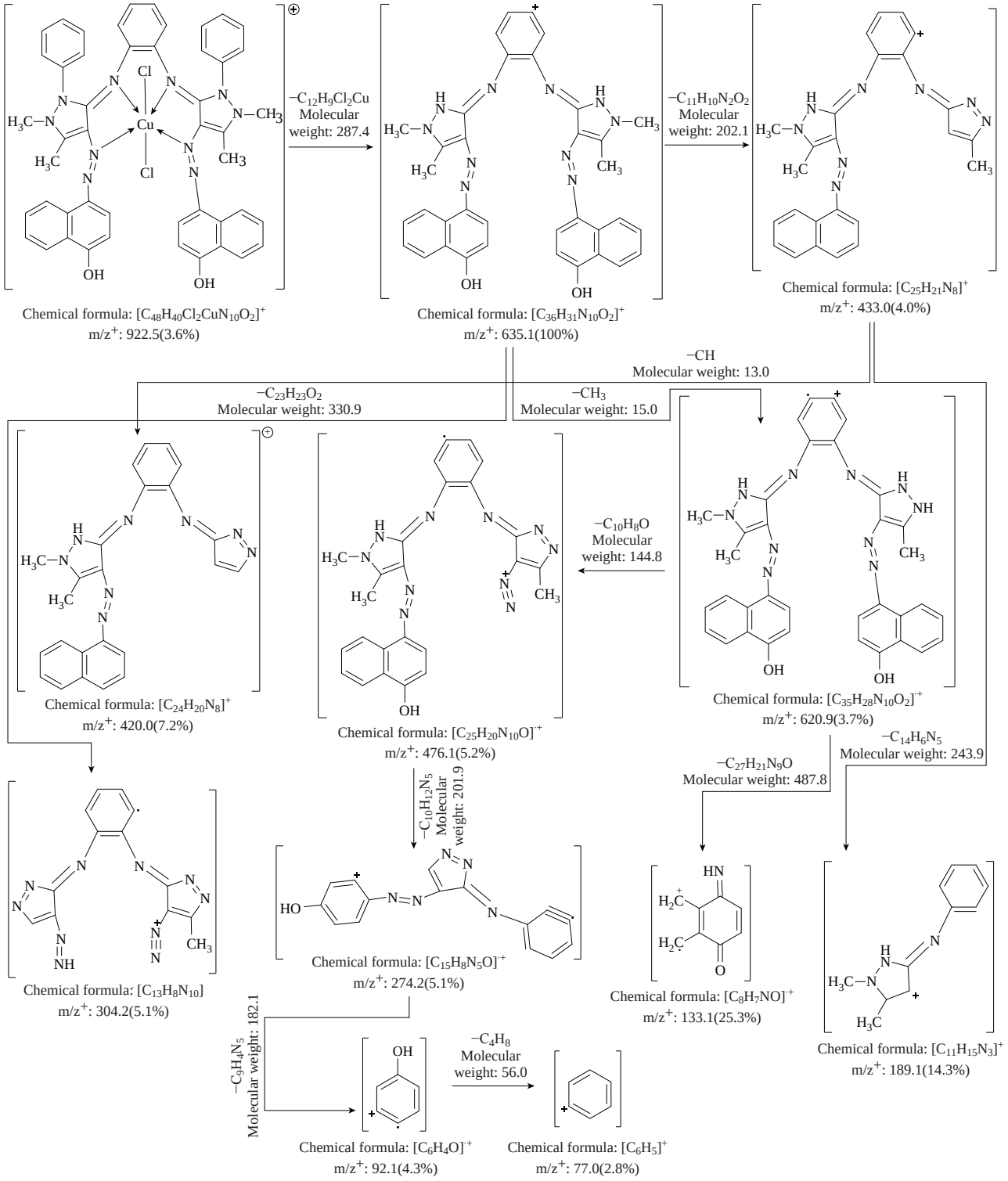

Scheme 4 Mass spectrum fragmentation of Cu- complex.

in Fig. 3.

^{13}C-NMR spectra

The ^{13}C-NMR spectra of the azo Schiff-base ligand were measured at room temperature in DMSO-d6 as a solvent. The spectra of the ligand are shown in Fig. 4. The ^{13}C-NMR spectrum of the ligand displayed characteristic signals at 11.3, 39.3,89 and 155.3 ppm due to >C–CH3, >N-CH_3, >C-N=N- antipyrine ring and >C-OH naphthol ring of the Schiff base-azo ligand, respectively [8, 23]. The peak at δ = 163.3 ppm was due to azomethine carbon of the ligand [8]. Moreover, the spectrum of the ligand showed peaks in the region of 108.2, 109.9, 111.09, 122.1, 126.6, 127.6, 129.01 and 140.9 ppm due to aromatic carbon atoms.

Electronic spectra

Electronic spectra provided the most detailed information about the electronic structure. The UV-Vis spectrum of the azo Schiff-base ligand exhibited two charge transfer (CT) bands at 316 nm 31645/cm and 412 nm 24271/cm, which was attributed to π–π* and n– π* transitions within the azo Schiff-base ligand. In the spectrum of the complexes, the CT band at 316 nm remained as such, in agreement with the π–π* transition of the azo Schiff-base ligand. The band observed at 412 nm in the spectrum of the free ligand (HL) was red-shifted to 449-549 nm in the complexes due to ligand to metal charge transfer (LMCT) transition [24], suggesting an octahedral geometry around metal(II) in the complexes [25]. The electronic spectra of the ligand and the Cu(II) complex are shown in Fig. 5. The electronic transitions, magnetic properties and conductivity values of the ligand and its complexes are listed in Table 4.

Magnetic measurements

The Fe(III) complex showed magnetic value at magnetic effect (μeff) = 5.4 B.M, which was consistent with an octahedral geometry [26]. The Co(II) complex had a magnetic moment of 4.91 BM, which was in agreement with the reported value for octahedral Co(II) complexes [27]. The present Ni(II) complex showed a magnetic moment value of 3.1 within the range of 2.9-3.3 BM [25, 28], suggesting an octahedral environment. The Cu(II) complex showed a magnetic moment value of 1.82 BM, higher than the spin-only value 1.73 BM as expected for one unpaired electron, which was monomeric and consistent with a distorted octahedral geometry [29]. The Zn(II), Cd(II), Hg(II), Au(III) were diamagnetic and according to the empirical formulae of complexes. An octahedral geometry was proposed [30], except the Au(III) complex suggested a square planar geometry around the central metal ion [31]. Based on the above

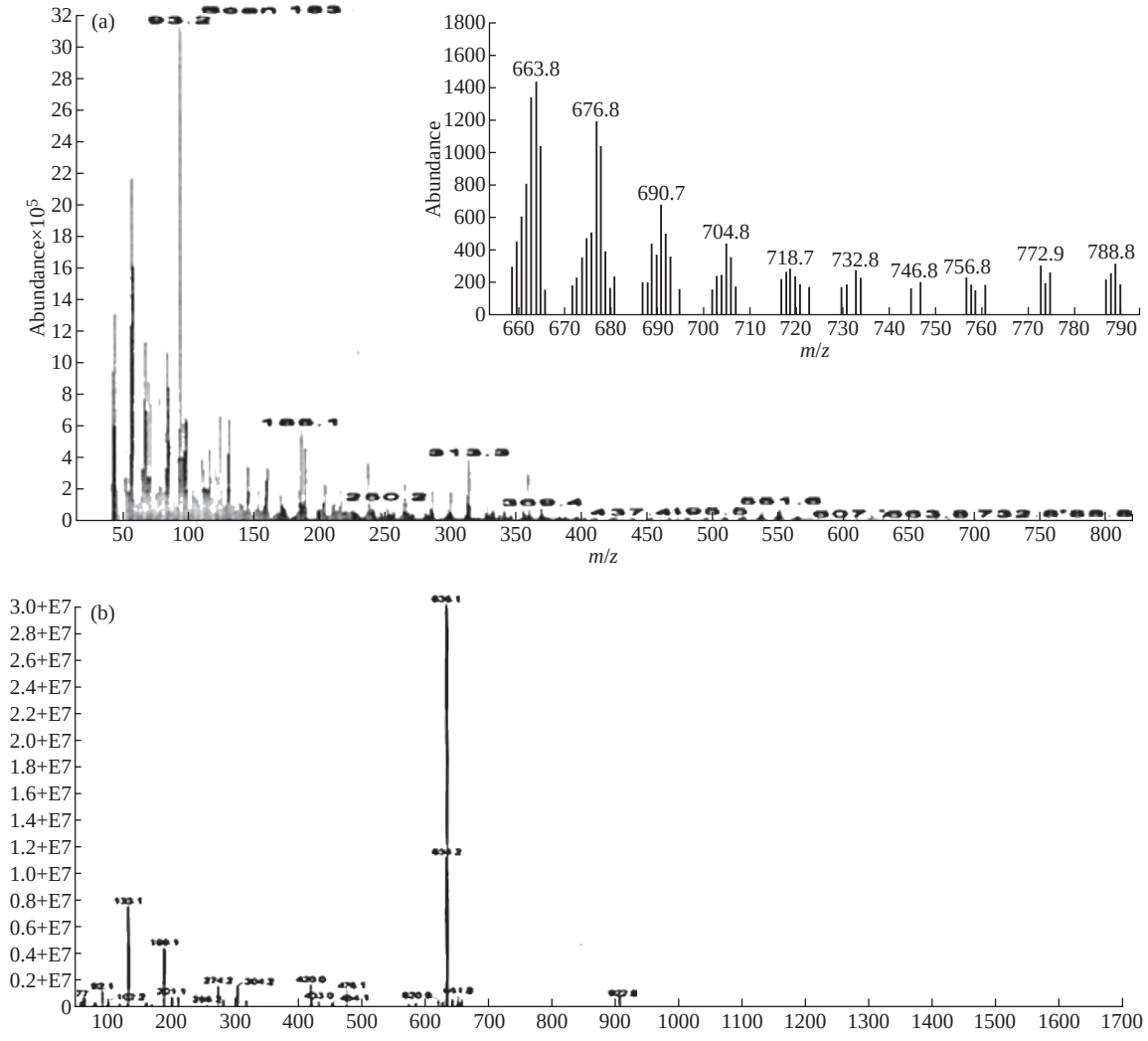

Fig. 2 Mass spectrum of **(a)** azo Schiff-base ligand and **(b)** Cu (II) complex.

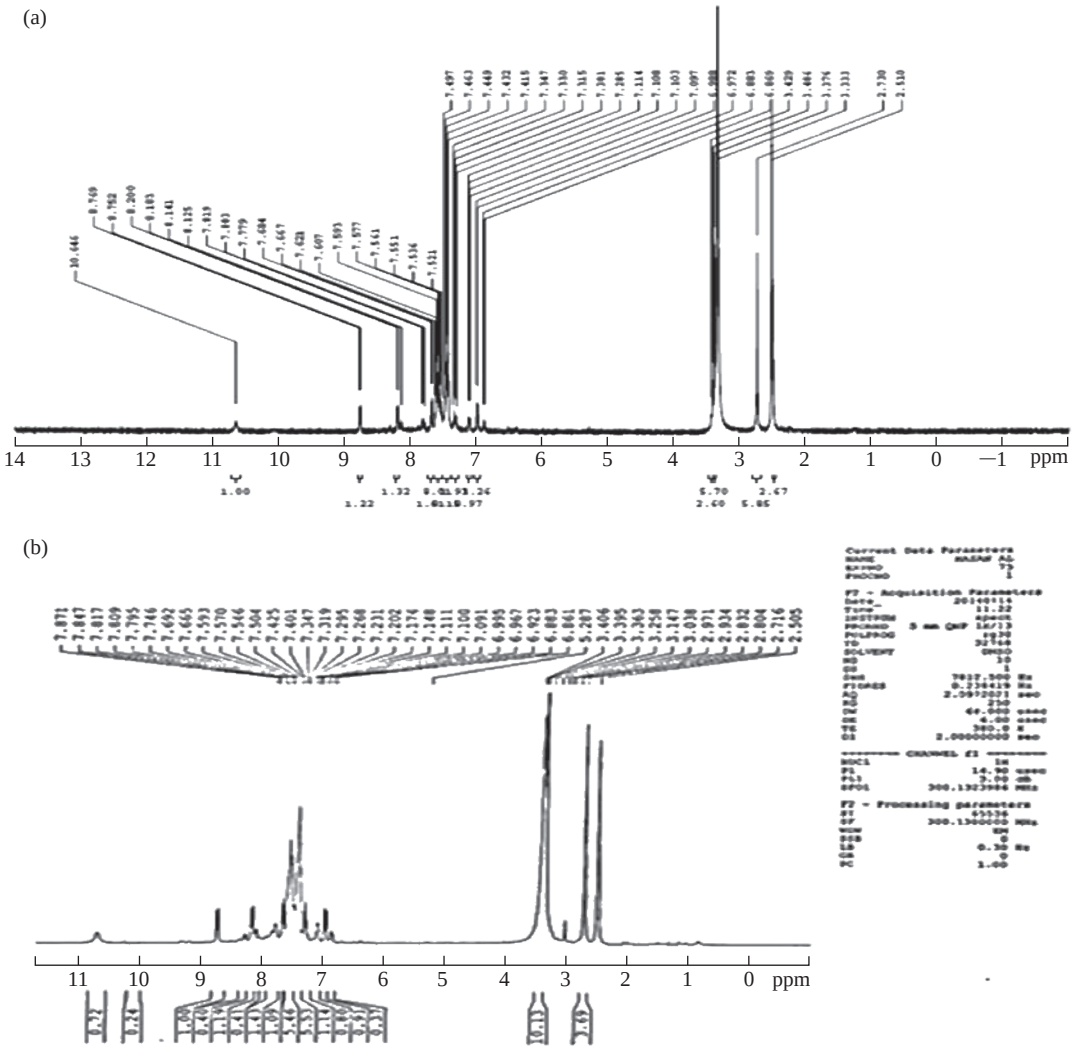

Fig. 3 [1]H-NMR spectrum of **(a)** azo Schiff-base ligand and **(b)** Zn (II) complex.

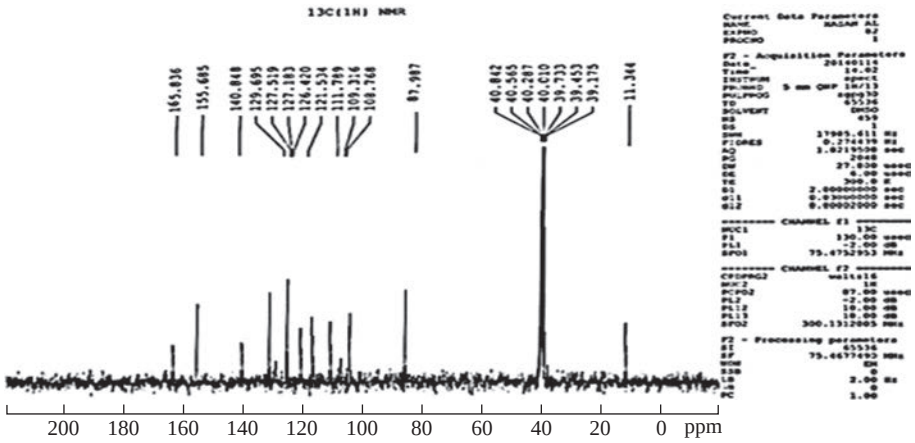

Fig. 4 [13]C-NMR spectrum of the azo Schiff-base ligand.

results, we could deduce the probable structures of the complexes as shown in Fig. 6.

Anticancer activity

Evaluation of newly synthesized complexes in cancer therapy were studied. In this study the antitumor activities of the synthesized Au(III) complex were tested against colon cancer (disease: Dukes' type B, colorectal adenocarcinoma) LS174 cell line. The results showed that the highest inhibitory effect was reported for complex, giving the IC50 value as of 465. The cell cytotoxic effect of the tested Au(III) complex

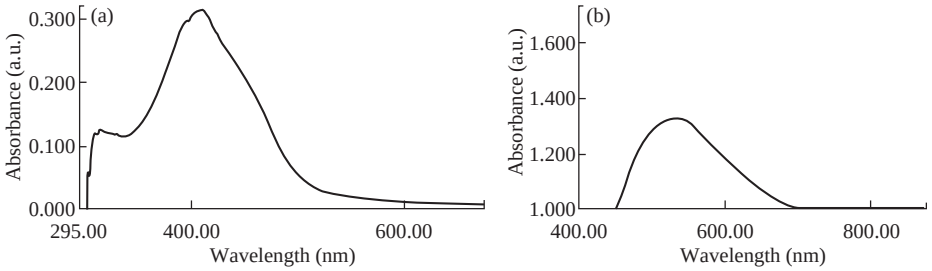

Fig. 5 Electronic spectrum of **(a)** ligand and **(b)** Cu(II) complex.

Table 4 Electronic spectra, conductivity and magnetic moment of complexes

Compound	Absorption Bonds (nm)	Absorption Bonds (/cm)	Transition	μeff (BM)	Conductivity (S cm^2/mol)	Geometry	Hybridization
H(L)	316 412	31645 24271	π → π * n → π *	--	--	--	--
$Fe(L)Cl_2Cl$	512	19531	M → L,CT	5.4	35	Octahedral (regular)	sp^3d^2
$Co(L)Cl_2$	549	18214	M → L,CT	4.91	9	Octahedral (distorted)	sp^3d^2
$Ni(L)Cl_2$	449	22271	M → L,CT	3.1	15	Octahedral (regular)	sp^3d^2
$Cu(L)Cl_2$	539	18552	M → L,CT	1.82	12	Octahedral (distorted)	sp^3d^2
$Au(L)Cl_3$	540	18518	M → L,CT	Diamagnetic (Dia)	195	Square- planar	dsp^2
$Zn(L)Cl_2$	508	19685	M → L,CT	Dia	6	Octahedral (regular)	sp^3d^2
$Cd(L)Cl_2$	512	19531	M → L,CT	Dia	13	Octahedral (regular)	sp^3d^2
$Hg(L)Cl_2$	516	19379	M → L,CT	Dia	11	Octahedral (regular)	sp^3d^2

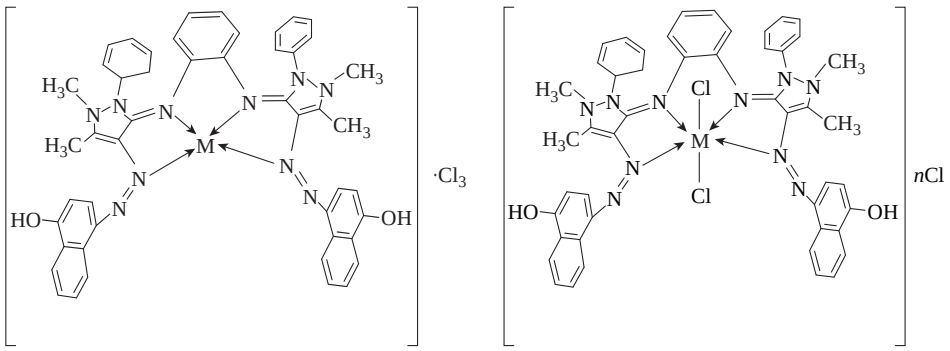

Fig. 6 Proposed structural formulae of the complexes.

was calculated. The optical density was measured with the micro plate reader to determine the number of viable cells, and the percentage of viability was calculated as

$$[1-(ODt/ODc)] \times 100\%, \quad (1)$$

where ODt is the mean optical density of wells treated with the tested sample and ODc is the mean optical density of untreated cells. The relation between surviving cells and drug concentration was plotted to get the survival curve of each tumor cell line after treatment with the specified complex. The 50% inhibitory concentration (IC50), the concentration required to cause toxic effects in 50% of intact cells, was estimated from graphic plots of the dose response curve for each concentration using Graph pad Prism 6. The anticancer activity of the synthesized Au(III) complex was determined against an colon cancer LS-174 cell line using different concentrations, evaluated and compared with the standard drug doxorubicin (DOX). The gold complex exhibited good results compared with the standard DOX. The in-vitro inhibitory activity of the tested gold complex against colorectal carcinoma LS-174 cells was expressed as

IC50 value (μg/mL). The results are shown in Table 5, 6, Fig. 7 and 8. The cytotoxicity of Au(III) complex on normal cells, i.e. rat embryo fibroblast cell line (REF) was studied using methyl thiazolyl tetrazolium (MTT) assay. The results indicated the effect of toxicity was very low. The results are shown in Fig. 9. The positive charge of the metal increased the acidity of coordinated ligand that bore protons, leading to stronger hydrogen bonds which enhanced the biological activity [32]. Moreover, Gaetke and Chow had reported that, metal has been suggested to facilitate oxidated tissue injury through a free-radical mediated pathway analogous

Table 5 The percentage of inhibition and Log x for the Au(III) complex

x = conc. (μg/mL)	0.5	1	10	100	1000	2000	3000	4000	5000	10000
Log x	0	0	1	2	3	3.3	3.5	3.6	3.7	4
Inhibition (%)	14.7	18.8	24.9	26.5	26.9	34.6	44.5	61.5	64.5	66.0
y = 40.35; Log IC50 = 2.668; IC50 = 465.58										

Note: Conc. = concentration; y = statistical value; IC50 = 50% inhibitory concentration.

Table 6 The percentage of inhibition and Log x for the DOX drug

x = conc. (μg/mL)	0.5	1	10	100	1000
Log x	0	0	1	1.7	2
Inhibition (%)	24.6	25.8	27.6	35.1	50.4
y = 37.5; Log IC50 = 1.503; IC50 = 31.8					

Note: Conc. = concentration; y = statistical value; IC50 = 50% inhibitory concentration.

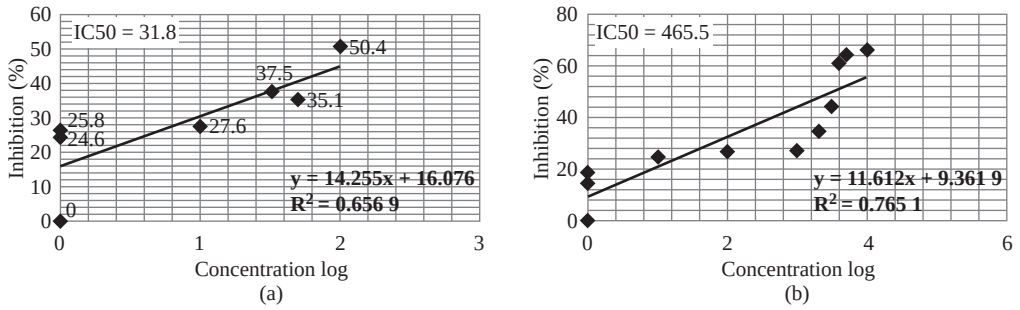

Fig. 7 Curve with plotting of lC50 of **(a)** doxorubicin drug and **(b)** Au(III) complex.

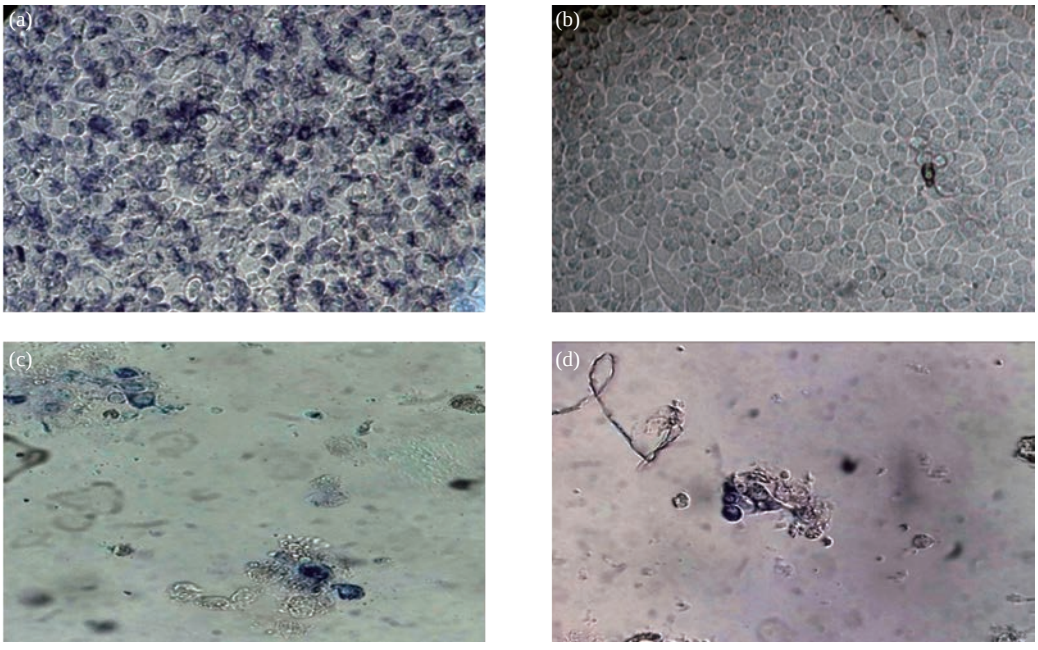

Fig. 8 **(a)** Untreated cell with MTT; **(b)** untreated cells; **(c)** and **(d)** treated cells with gold complex in conc. = 1000 and 2000 μg/mL.

to the Fenton reaction [33]. By applying the electron spin resonance (ESR trapping technique, evidence for metal-mediated hydroxyl radical formation in vivo has been obtained [34]. Reactive oxygen species (ROS) was produced through a Fenton-type reaction as follows:

$$LM(II) + H_2O_2 \rightarrow LM(I) + .OOH + H^+, \quad (2)$$

and

$$LM(I) + H_2O_2 \rightarrow LM(II) + .OH + OH^-, \quad (3)$$

where L refers to the organic ligand.

Also, metal could act as a double-edged sword by inducing DNA damage and also by inhibiting their repair [35]. The OH radicals reacted with DNA sugars and bases, and the most significant and well-characterized of the OH reactions was hydrogen atom abstraction from the C4 on the deoxyribo to yield sugar radicals with subsequent β-elimination (Scheme 5). By this mechanism strand break occurred as well as the release of the free bases. Another form of attack on the DNA bases was by solvated electrons, probably via a similar reaction to those discussed below for the direct effects of radiation on DNA [35].

Conductivity measurement

Most of the chelate complexes prepared in this work showed the conductivity values ranged between 73-80 S cm^2/mol in DMSO at room temperature, which were very low values [25] compared with the high values of conductivity of both Au(III) and Fe(III) complexes [31]. This could support the electrolytic nature of the metal complexes.

According to these results, the structural formulae of these ligand and complexes may be proposed in Fig. 6.

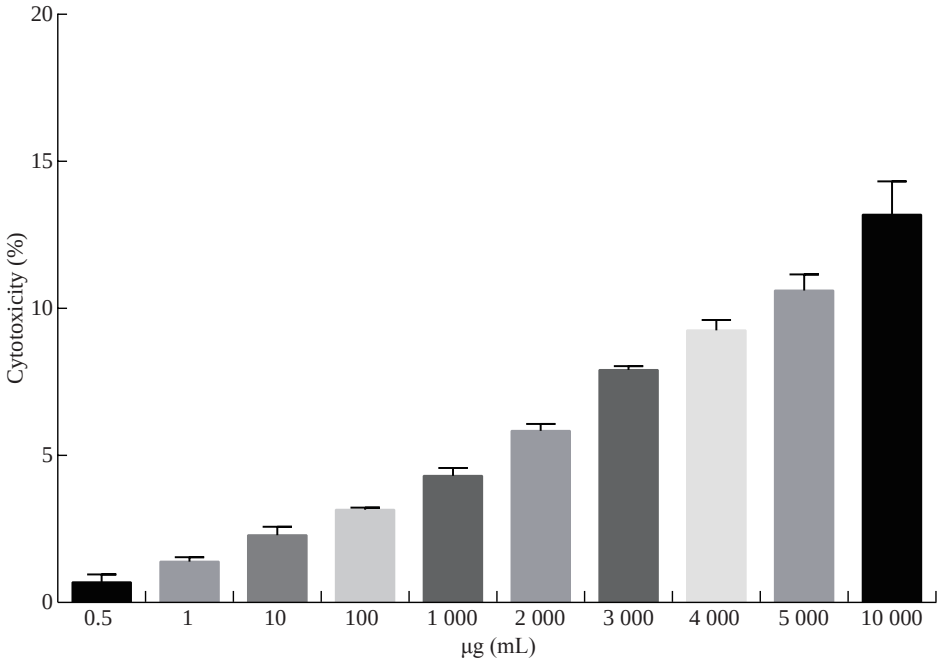

Fig. 9 Determination of the cytotoxic effect on REF.

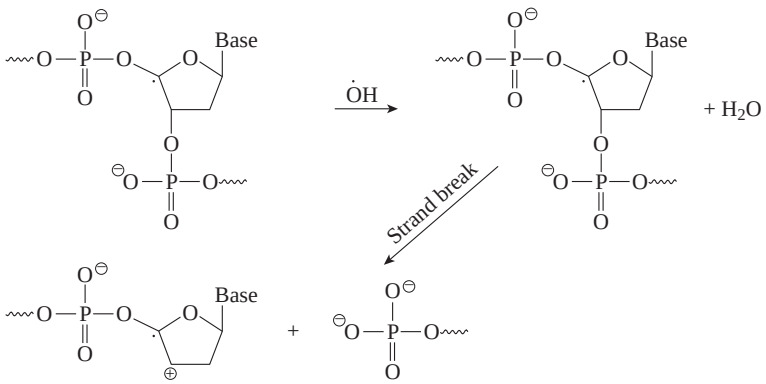

Scheme 5 Mechanism of Fenton reaction.

Conclusions

In this paper we explored the synthesis and coordination chemistry of some monomeric complexes obtained from the reaction of the tetra dentate ligand (L) with some metal ions as shown in Fig. 6. The mode of bonding and the overall structure of the complexes were determined through physico-chemical and spectroscopic methods. Complex formation study via molar ratio was investigated and results were consistent with those found in the solid complexes with a ratio of M : L = 1 : 1. The biological screening effect of the gold complex was tested against human colon cancer cell line LS-174. The results showed the highest inhibitory effect for the complex.

Conflict of Interests

The authors declare that no competing interest exists.

References

[1] A.A. Al-Hamad, S.A. Shaker, Synthesis, characterization, structural studies and biological activity of a new Schiff base-azo ligand and its complexation with selected metal ions. *Oriental Journal of Chemistry*, 2011, 27(3): 835-845.

[2] I.N. Witwit, H.A. Mohamad, Synthesis and spectral study of new tetradentate Azo-methine ligand as adrevitave of 4, 5-diphenyl Imidazole and its complexes with some of metal Ions. *Journal of the Faculty of Basic Education*, 2016, 95: 1-12.

[3] L.A. Mohamad, R.A. Albaki, H. Mohseen, et al., Synthesis, characterization, structural studies and Biology activity of a new macrocyclic Schiff base ligand and it's complexation with selected metal Ions. *Journal of scientific Research in Pharmacy*, 2013, 2(3): 7-13.

[4] P. Pattan Ayak, D. Patra, J. Pratihar, et al., Osmium and cobalt complexes in corporating facially coordinated N,N,O donor azo-imine ligands: Redox and catalytic. *Properties. J. chem. Sci*, 2013, 125(1): 51-62.

[5] D.M. Jamil1, A.K. Al-Okbi, S.B. Al-Baghdadi, et al., Experimental and theoretical studies of Schiff bases as corrosion inhibitors. *Chemistry Central Journal*, 2018, 12(7): 1-7

[6] C. Anitha, S. Sumathi, P. Tharmaraj, et al., A new azo-schiff base: Synthesis, chaactrization biological activity and theoretical studies of its complexes. *Applie Organo Metallic Chem*, 2018, 32: 1 -15.

[7] M.A. Karam, H.D. Salman, Synthesis, characterization and antimicrobial studies of transition metal complexes with azo ligand derivative from 4-amino antipyrine. *Mesopo. Environ. J.*, 2017, Special Issue C: 83-91

[8] N. Srividhya, A. Xavier, Antimicrobial activities of Schiff base metal complexes of 4-amino antipyrine. *International Journal of Research in Engineering and Advanced Technology*, 2017, 4(6): 28-35.

[9] N.G. El-Kholy, Synthesis, spectroscopic characterization, antimicrobial, antumor properties of new 4-amino-2,3 dimethyl-1-pheny-3-pyrazolone-5-one (antipyrine) Schiff bases and its transition metal complexes. *Journal of American Science*, 2017, 13(2): 132-145.

[10] G. Turan-Zitouni, M. Sivaci, Synthesis of some trizolyl-antipyrin derivatives and investigation of analgesicactivity. *Eur. J. Med. Chem.*, 2001, 36(8): 685-689.

[11] A.N. Lutsevich, K.I. Bender, and O.V. Reshetko, The relationship between antipyrine kinetics, the seromucoid content and the xanthine oxidase activity in the plasma of rats with acute and chronic in flammation. *Ekspklin Farmakol*, 1995, 59: 51-55.

[12] M.S. Karan, D. Arish, and J. Johnson, Synthesis, characterization and biological studies on some metal complexes with Schiff base ligand containing pyrazolone moity. *J. of Saudi Chem. Soc.*, 2016, 20: 591-598.

[13] M.A. Metwally, M.A. Gouda, A.N. Harmal, et al., Synthesis, antitumor, cytotoxic and antioxidant evaluation of some new pyrazolo triazines attached to antipyrine moiety. *Eur. J. Med. Chem.*, 2012, 56: 254-262.

[14] A. Accardo, L. Alo, and M. Aurilio, Receptor binding peptides for target-selective delivery of nano particles encapsulated drugs. *Int. J. Nano Medicine*, 2014: 1537-1557.

[15] S.R. Jumar, Anticancer activity of eco-friendly gold nano particles against lung and liver cancer cells, *Journal of Genetic Engine erring and Biotechnology*, 2016, 14: 195-202.

[16] K.J. Al-Adilee, Preparation and characterization of some transition metal complexes with novel Azo-schiff base ligand derived from 2(E)-(1H-benzo) [d] imidazole-2-ylydiazenyl)-5-(E)-benzylidene imino) phenol (BIADPA). *Pharmaceutical, Biological and Chemical Sciences*, 2015, 6(5): 1297-1285.

[17] M.B. Ummathur, P. Sayunderi, and K. Kuutty, Schiff bases of 3-[2-(193-Benzothiazol-2-yl] hydrazinyliene] pentane-2,4-dione with aliphatic diamines and their metal. *Journal of the Argentine Chemical Society*, 2009, 97(2): 31-39.

[18] D. Çanakçi, O.Y. Saribiyik, and S. Serin, Synthesis, structural characterization of Co(II), Ni(II) and Cu(II) complexes of azo dye ligand derived from dihydroxy naphthalene. *International Journal of Scientific Research and Inovative Technology*, 2014, 1(2): 91-107

[19] N. Raman, S. Thalamuthu, J. Dhaveethuraja, et al., DNA cleavage and antimicrobial activity studies on transition metal (II) complexes of 4-amino-antipyrine derivative. *J. Chil. Chem. Soc*, 2008, 53(1).

[20] B.K. Al-Salami, R.A. Gata, and K.A. Asker, Synthesis spectral, thermal stability and bacterial activity of schiff base derived from selective amino acid and their complexes. *Pelagia Research Libray*, 2017, 8(3): 4-12.

[21] S.D. Dakore, V. Kamble, and P. Bisal, Synthesis and characterization of biologically active N_2O_2 type of Novel Schiff base metal complexes derived from 4-aminoanty pyrine using TEA. *J. Chem Studies*, 2017, 5(1): 110-113.

[22] M.Y. Nassar, I.S. Ahmed, H.A. Dessouki, et al., Synthesis and characterization of some Schiff base complexes derived from 2, 5-dihydroxyacetophenone with transition metal ions and their biological activity. *Environ. Sci.*, 2018, 5: 60-71

[23] L.M.L. Ogboji, O.Z Esezobor, Synthesis of 4,4'-dihydroxyazo benzene and 4'dihydroxyphenyl azo-2-naphthol from diazotised aniline and anthocyanins from diazotised aniline and anthocyanins from delonix regia flower. *Chemical Science International Journal*, 2017, 20(1): 1-5

[24] Z.J. Mohamed, A.H. Al-Khafagy, Characterization and Biological study of heterocyclic azo-schiff base compound and some of its metal complexes. *International*

Journal of Current Research, 2013, 5(12): 3705-3710.
[25] M.S. Mohamad, Some transition metal complexes with new Schiff base ligand hexa dentate. *Acta Chimica Pharm Indica*, 2013, 3(2): 140-148.
[26] M.K.P. Shree, S. Vats, Schiff base and Transition metal complexes. *J. Biol. Chem. Sci.*, 2016, 3(2): 265-300.
[27] S.H. Kadhim, I.Q. Abd-Alla, and T.J. Hashim, Synthesis and characteris study of Co(II), Ni(II), and Cu(II) complexes of new Schiff base derived from 4-amino antipyrine. *Inte. J. Chem. Sci.*, 2017, 15(1): 107.
[28] R.M. El-Ferjani, M. Ahmad, F.W. Harum, et al., Synthesis, characterization and antibacterial activity of Schiff base derived from 4-Dimethyl amino benzaldehyde with some amino acids and 4-amino antipyrine toward Cu(II), (Ni(II), Co(II), Cd (II) and Mn (II) ions. *Journal of Applied Chemistry*, 2017, 10(6): 6-13.
[29] E. Yousif, A. Majed, and K. Al-Summarrae, Metal complexes of Schiff base: preparation, characterization and antibacterial activity. *Arabian Journal of Chemistry*, 2013: 2006-2012.
[30] M. Suresh, V. Prakash, Preparation and characterization of Cr(II), Mn(II), Co(II), Ni(II), Cu(II), Zn(II) and Cd(II) chelates of Schiff bases derived from vanillin and 4-amino antipyrine. *Inter. J. Physical Sci.*, 2010, 5(4): 2203-2211.
[31] P. Deshmukh, P.K. Soni, A. Kankoriya, et al., 4-Amino antipyrine: A significant tool for the synthesis of biologically active Schiff base and metal complexes. *Int. J. Pharm. Sci, Rev.*, 2015, 34(1): 162-170.
[32] B. Bauer-Siebenlist, F. Meyer, E. Farkas, et al., Effect of Zn...Zn separation on the hydrolytic activity of model dizinc phosphodiesterases. *J. Chem. Eur.*, 2005, 11: 4349-4360.
[33] L.M. Gaetke, Copper toxicity, oxidative stress, and antioxidant nutrients. *J. Toxicology*, 2003, 189: 147-163.
[34] D.E. Nikles, M.J. Powers, Copper(II) complexes with tetradentate bis(pyridyl)-dithioether and bis(pyridyl)-diamine ligands. Effect of thio ether donors on the electronic absorption spectra, redox behavior, and EPR parameters of copper(II) complexes, *Inorganic Chem.*, 1983, 22: 3210-3217.
[35] C.A. Rouzer, Some transition metal complexes with new Schiff base ligand hexa dentate. *Acta Chimica J. Chem. Res. Toxicol*., 2010, 23: 1517-1518.